Tunnelling system coupled to a harmonic oscillator: an analytical treatment

Tunnelling system coupled to a harmonic oscillator: an analytical treatment

S Paganelli[1] and S Ciuchi[2]

[1] Dipartimento di Fisica, Università di Roma La Sapienza, P. A. Moro 2, I-00185 Rome, Italy
[2] Dipartimento di Fisica, Università dell'Aquila, Via Vetoio, I-67100 L'Aquila, Italy

Abstract
We give an analytical formula in term of continued fraction expansions for the
spectral function of a tunnelling electron, coupled to a local lattice oscillation, in
a two-site cluster at non-zero temperature. We also study the spectral function
of the polaron, a better defined quasi-particle in the anti-adiabatic regime and
at sufficiently low temperature. The exact results obtained allow us to look
into a wide range of temperature and coupling. Asymptotic results can be
obtained directly from the continued fraction expansions in both adiabatic and
anti-adiabatic regimes. In the intermediate/strong anti-adiabatic case, in contrast
to the usual Lang–Firsov approximation scheme, we found that there is no
shrinking of the polaron band as temperature increases. Polaron bandwidth gets
broader by temperature effects.

(Some figures in this article are in colour only in the electronic version)

1. Introduction

Tunnelling of a charge between localized sites, in a crystal or a molecular system, can be
severely affected by coupling with optical phonon modes. The competition between kinetic
energy of the charge and localization effects due to local coupling with phonon produces the
small polaron, i.e. a charge dressed by a cloud of multiphonon processes, when the latter
prevails.

To have a *small* polaron we thus must have a short-range electron–phonon interaction
and narrow bands [1, 2]. In fact, if the crystal can be considered as made of strongly
deformable molecular-like units with narrow-band electrons hopping from one to another, then
the conditions for a strong polaron effect can be achieved [2]. In realistic structures, for example
transition metal oxides or organic metals, such units exist which provide local (oscillation)
phonon modes and are indeed strongly coupled to well defined electronic orbitals.

The concept of small polaron, introduced in the aforementioned cases of solid state
physics, is also relevant in the physics of organic materials. In this case, molecular units
leading to very narrow bands are easily realized, e.g. the case of organic polymers [3] in which

bandwidth is of the order of eV. In the case of sufficiently pure acene crystals [4], very narrow bands are also found, due to extremely weak Van Der Waals forces between the molecular units. Here the typical bandwidth is of the order of few hundreds of meV. In these compounds we can approach the anti-adiabatic regime—in which phonon frequencies becomes of the order of the bandwidth—inaccessible in solid state physics. Small polaron effects have been recently invoked to explain exciton motion in photosynthetic light-harvesting systems [5] and charge motion in DNA [6, 7]. In these cases 'bands' are so narrow and 'disorder' due to the presence of different kind of molecular units (e.g. bases in DNA) is so large that at room temperature the motion is essentially hopping-like and localization effects are very important.

For these reasons, it is interesting to span the largest region of coupling constant strength as well as phonon frequency and temperature to characterize the polaron formation which occurs as a crossover [8] in all regimes.

To accomplish this task, we study, with analytical methods, dynamical properties of a two-site cluster which is the minimal system in which competition of hopping between two sites and phonon localization effects takes place. This competition is crucial to describe properly the polaron crossover as a function of the electron–phonon coupling constant. For this reason the two-site systems have been extensively studied since the pioneering work of Holstein [2]. Ground state properties [9–13] along with spectral properties [16, 9, 14, 15] have been studied using both numerical [9, 14, 10] as well as analytical methods [16, 12, 13]. Also for its simplicity, the two-site cluster has been studied in more involved problems, such as polaron formation in the presence of double exchange [17] or in the presence of on-site electronic repulsion [18]. It is worth mentioning also the relevance of the two-site system in the high temperature case, where the coherence is lost in a single tunnelling [19]. The two-site system can also form the building block for a cluster approximation [20].

In this paper, we shown an analytical method that can be applied in the non-zero temperature case, which was formerly investigated by the path integral approach [21]. We obtain electron spectral properties, as well as the phononic displacement distribution function, and we compare this information to investigate the polaron crossover as a function of the various parameters and of the temperature. We also compare electron and polaron Green functions to quantitatively determine whether the polaron is the tunnelling quasi-particle, and how the temperature affects these dynamical properties.

The paper is organized in sections. The model is introduced in section 2 and solved in section 3. In section 4 are reported the results at $T = 0$ and $T > 0$ respectively. Section 5 is devoted to conclusions. Appendices report the calculations.

2. The model and its limiting regimes

The model describes an electron, in the tight binding approximation, moving in a two-site lattice and interacting with it by the local distortion of the lattice site. The Hamiltonian is [11]

$$H = -J(c_1^\dagger c_2 + c_2^\dagger c_1) + \omega_0(a_1^\dagger a_1 + a_2^\dagger a_2) - g[c_1^\dagger c_1(a_1^\dagger + a_1) + c_2^\dagger c_2(a_2^\dagger + a_2)] \tag{1}$$

$c_j^\dagger$ and $a_j^\dagger$ are, respectively, the electron and phonon creation operators. The strength of the electron–phonon interaction is given by the constant g, J is the electron hopping integral and $D = 2J$ is the tight binding half-bandwidth. Here we only consider one dispersionless phonon per site with frequency ω_0.

We can reduce the degrees of freedom introducing the coordinates corresponding to the centre of mass and the relative displacement. The centre of mass Hamiltonian consists in a displaced oscillator and can be separated from the part depending on the relative coordinate $(a = (a_1 - a_2)/\sqrt{2})$. In the following discussion we shall limit ourselves to study only the

latter

$$H = \omega_0 a^\dagger a - J\sigma_x - \tilde{g}\sigma_z(a^\dagger + a). \tag{2}$$

In (2) $\tilde{g} = g/\sqrt{2}$ and a pseudo-spin notation has been used by introducing the Pauli matrices $\sigma_z = c_1^\dagger c_1 - c_2^\dagger c_2$ and $\sigma_x = c_1^\dagger c_2 + c_2^\dagger c_1$.

The Hamiltonian (2) has a very general form and, even if it has been derived for a two-site cluster, it is suitable to describe a very wide class of problems (for example a two-level system interacting with a single optical mode [16]).

Beside the temperature, we can choose two parameters that characterize the model: (i) the bare e–ph coupling constant $\lambda = g^2/(\omega_0 J)$ given by the ratio of the polaron energy ($E_p = -g^2/\omega_0$) to the hopping J and (ii) the adiabatic ratio $\gamma = \omega_0/J$. In terms of these parameters we can define weak coupling $\lambda < 1$ and strong coupling $\lambda > 1$ regimes as well as adiabatic $\gamma < 1$ or anti-adiabatic $\gamma > 1$ regimes. Notice that, in the so called atomic ($J = 0$) limit, the coupling's strength is better described by another constant, i.e. $\alpha = \sqrt{\lambda/(2\gamma)}$.

In the atomic limit the Hamiltonian is diagonalized by the so-called Lang–Firsov (LF) transformation [22]

$$D = e^{\alpha\sigma_z(a^\dagger - a)}. \tag{3}$$

This transformation shifts the phonon operators by a quantity α, while the electron operator is transformed into a new fermionic one associated with a quasi-particle, called a polaron, with energy E_p. It can be shown that α^2 is the mean number of phonons in the polaron cloud.

By applying the LF transformation $\bar{H}_0 = D^\dagger H_0 D$, the atomic Hamiltonian $H_0 = \omega_0 a^\dagger a - \tilde{g}\sigma_z(a^\dagger + a)$ becomes

$$\bar{H}_0 = \omega_0 a^\dagger a + E_p/2, \tag{4}$$

the eigenvalues $E_n = \omega_0 n + E_p/2$ correspond to the twofold degenerate eigenvectors $|\psi_n^j, j\rangle = D|n, j\rangle = \bar{c}_j^\dagger|n\rangle$, where the index $n = 0, \ldots, \infty$ refers to the phonon number, $j = 1, 2$ to the electron site number and $\bar{c}_j^\dagger$ is the polaron creation operator $\bar{c}_j^\dagger = Dc_j^\dagger D^\dagger = c_j^\dagger \exp\{(-1)^j\alpha(a^\dagger - a)\}$.

In the case of finite J, the hopping term is not diagonalized by (3) and the new Hamiltonian $\bar{H} = D^\dagger H D$ becomes

$$\bar{H} = \omega_0 a^\dagger a - J(\sigma_x \cosh(2\alpha(a^\dagger - a)) + i\sigma_y \sinh(2\alpha(a^\dagger - a))) + E_p/2. \tag{5}$$

Depending on the choice of the parameters, the problem could be better described by an electron or polaron excitation picture. In particular, in the weak coupling limit, both the small polaron and the electron are good quasiparticles while, in the intermediate and strong coupling regimes, the polaron behaviour prevails [23]. For this reason it is useful to consider the spectral properties of both particles.

We consider the following electron Green's function:

$$G_{i,j}^{(\text{el})}(t) = -i\theta(t) \sum_n \frac{e^{-\beta\omega_0 n}}{Z_0} \langle n|c_i(t)c_j^\dagger|n\rangle \tag{6}$$

or, explicitly,

$$G_{i,j}^{(\text{el})}(t) = -i\theta(t)(1 - e^{-\beta\omega_0}) \sum_n e^{-\beta\omega_0 n} \langle n; 0|c_i e^{-i(H-\omega_0 n)t} c_j^\dagger|0; n\rangle \tag{7}$$

where $Z_0 = (1 - e^{-\beta\omega_0})^{-1}$ is the phonon partition function. $G^{(\text{el})}$ measures the amplitude of the process in which an electron is initially injected into site j and then destroyed at time t on site i.

In a similar way we can introduce a polaron Green's function by creating and destroying a polaron

$$G_{i,j}^{(pol)}(t) = -i\theta(t) \sum_n \frac{e^{-\omega_0 n\beta}}{Z} \langle n|\bar{c}_i(t)\bar{c}_j^\dagger|n\rangle \tag{8}$$

or

$$G_{i,j}^{(pol)}(t) = -i\theta(t)(1 - e^{-\beta\omega_0}) \sum_n e^{-\omega_0 n\beta} \langle n|c_i e^{-i(\bar{H}-\omega_0 n)t} c_j^\dagger|n\rangle. \tag{9}$$

Another meaningful quantity is the phonon distribution, defined as

$$P(x) = \frac{1}{Z}\text{tr}[e^{-\beta H}|x\rangle\langle x|] \tag{10}$$

in this case Z is the partition function of the whole system. In term of this function we can characterize the polaron crossover as given by the transition between a monomodal and a bimodal $P(x)$ [17, 24, 25].

Let us consider separately the adiabatic and anti-adiabatic regimes. The anti-adiabatic case was first studied in the small J perturbation regime [2, 26] and in the Holstein-Lang–Firsov approximation (HLFA) [2, 22], where an effective Hamiltonian is introduced to eliminate the phonon states. In HLFA, J is substituted by an effective hopping integral, obtained by averaging the displacement $\exp[2\alpha(a^\dagger - a)]$ on the thermal distribution of phonons. The resulting effective hopping integral is $\tilde{J} = J\exp(-2\alpha^2 \coth(\beta\omega_0/2))$. At zero temperature the well known exponential reduction of the bandwidth is obtained $\tilde{J} = J\exp(-2\alpha^2)$, while the more the temperature is increased ($T/J \gg \gamma$) the quicker the bandwidth decreases. This approximation is usually referred to the regime where the diagonal transitions (in which all the phonon occupation numbers remain the same during the hop) prevail. In this case, the inelastic processes are irrelevant and the motion of the quasiparticle remains coherent. We shall see that this is a good approximation at zero temperature but it becomes inadequate at finite T, where incoherent processes turn out to be important.

This fact was already pointed out in [14], where it was shown that, in the polaronic regime, the average kinetic energy, at low temperatures, goes up as temperature increases. In this paper we shall return to this point by studying the fermionic spectral functions, showing that at zero temperature the spectral weight is all concentrated in a renormalized band (here consisting in two poles only) according to the HLFA. As soon as the temperature increases, other poles appear, due to the incoherent scattering processes, while the original band remains exactly the same, even if its spectral weight diminishes. This means that renormalization of coherent processes is independent of temperature, but its cross section decreases till it becomes comparable to or smaller than the one of the incoherent processes.

It is important to notice that the HLFA refers only to the lower energy band. The vibrational degree of freedom gives rise, in the atomic limit, to a 'comb' of resonances corresponding to the excitation of a specific number of phonons. Each of these resonances is split in two as soon as the hopping is turned on. Obviously the HLFA does not say anything on the bandwidths of these higher energy resonances. For this purpose, a perturbative approach with respect to J can give a suitable indication (see appendix C). As we can see from (36) and (37), at $T = 0$ the poles are given by $\omega_m = \omega_0 m - \frac{g^2}{2\omega_0} \pm Jf_{m,m}(2\alpha)$, so the nth band has a width equal to

$$\tilde{J}_m = J|f_{m,m}(2\alpha)| = 2e^{-2\alpha^2}|L_m(4\alpha^2)| \tag{11}$$

where $\tilde{J}_0 = \tilde{J}$. It is interesting to notice that, for $f_{m,m}$'s sign being dependent on α, the eigenvalues of each band can cross each other (as stressed in [28, 27]). Is worth noting that the monotonic exponential decreasing of the bandwidth is only a feature of the first band, while in the higher energy cases a more complex behaviour appears.

The adiabatic case is another widely studied regime [11, 2, 26]. In the adiabatic limit ($\gamma = 0$) the eigenvalues of Hamiltonian (2) can be expressed through the classical displacement x

$$E_r^\pm(x) = \tfrac{1}{2}kx^2 \pm \sqrt{((g/\ell)^2 + J^2)} \tag{12}$$

where ℓ is the harmonic oscillator characteristic length and k the spring constant. The lowest branch ($-$) of (12) defines an adiabatic potential which has a minimum at $x = 0$ as far as $\lambda < 1$, while for $\lambda > 1$ it becomes a double well potential with minima at $x_0 = \ell\sqrt{2}\alpha$; in this case the electron is mostly localized on a given site. The quantum fluctuations are able to restore the symmetry in analogy to what happens for an infinite lattice [29]. It is worth noticing that, in this limit, Hamiltonian (2) is equivalent to the adiabatic version of the spin-boson Hamiltonian [30].

Even if the adiabatic approximation is a good description for a slow phonon, at very low temperature it does not take quantum fluctuations of phonons into account. This point will be widely examined later on.

In this work we present an exact solution also at finite temperature in every regime.

3. Diagonalization in the fermion space

As shown by Fulton and Gouterman [31], a two-level system coupled to an oscillatory system in such a manner that the total Hamiltonian displays a reflection symmetry may be subjected to a unitary transformation which diagonalizes the system with respect to the two-level subsystem [32, 33, 31]. This method can be generalized to the N-site situation, if the symmetry of the system is governed by an Abelian group [33].

In particular, an analytic method for solving the two-site Holstein model is given in [17]. Here the Hamiltonian is diagonalized in the electron subspace by applying a Fulton–Gouterman (FG) transformation to obtain a continued fraction expansion of the solution. In this framework, the analytical form for the electron Green functions was easily computed as well as the displacement probability distribution. Another continued fraction approach without FG transformation has been reported in [16].

In this section we generalize these results, extending them to the finite temperature case. Moreover, the polaron Green functions are studied by the introduction of another FG transformation. Even if this case is indeed formally solvable in the same way as the electron one, the final result is not suitable to be numerically implemented for an exponential increasing of its complexity. It will be thus useful to diagonalize the transformed Hamiltonian H_{LF}, instead of the original one, in the fermion subspace.

By applying the FG transformation

$$V = \frac{1}{\sqrt{2}} \begin{pmatrix} 1 & (-1)^{a^\dagger a} \\ -1 & (-1)^{a^\dagger a} \end{pmatrix}, \tag{13}$$

the new Hamiltonian $\tilde{H} = VHV^{-1}$ becomes diagonal in the electron subspace

$$\tilde{H} = \begin{pmatrix} H_+ & 0 \\ 0 & H_- \end{pmatrix} \tag{14}$$

the diagonal elements, corresponding to the bonding and antibonding sectors of the electron subspace, being two purely phononic Hamiltonians

$$H_\pm = \omega_0 a^\dagger a \mp J(-1)^{a^\dagger a} - \tilde{g}(a^\dagger + a) \tag{15}$$

with the eigenvalue equation associated

$$H_\pm |\phi_k^\pm\rangle = E_k^\pm |\phi_k^\pm\rangle. \tag{16}$$

The operator $(-1)^{a^\dagger a}$ is the reflection operator in the vibrational subspace and it satisfies the condition $(-1)^{a^\dagger a} a (-1)^{a^\dagger a} = -a$. The transformation (13) modifies the states as shown below

$$V|j;n\rangle = \frac{(-1)^{n(j-1)}}{\sqrt{2}} \left(|1\rangle + (-1)^j |2\rangle \right) |n\rangle \tag{17}$$

where $j = 1, 2$ denotes the site index. The set of eigenvectors of H is given by

$$|\psi_k^\pm\rangle = \frac{1}{\sqrt{2}} \left[(-1)^{a^\dagger a} |2\rangle \pm |1\rangle \right] |\phi_k^\pm\rangle. \tag{18}$$

A wide study of the eigenvalue problem was carried out in [27] both numerically and analytically by a variational method, extending the former results given in [28]. In [27] $H_\pm$ is approximatively diagonalized by applying a displacement, the dynamics is reconstructed by the calculated eigenvectors and energies.

Using the notation adopted in appendix A, we can expand the Fock states in the $H_\pm$ eigenvector basis

$$|n\rangle = \sum_\alpha \sqrt{\gamma_{\alpha,n}^\pm} |\phi_\alpha^\pm\rangle. \tag{19}$$

In this form the electron Green function can thus be expressed in terms of diagonal elements of the resolvent operator only, defined as

$$G_{m,n}^\pm(\omega) = \langle m| \frac{1}{\omega - H_\pm} |n\rangle. \tag{20}$$

More explicitly

$$G_{1,1}^{(\text{el})}(\omega) = \frac{(1 - e^{-\beta\omega_0})}{2} \sum_n e^{-\omega_0 n\beta} [G_{n,n}^+(\omega + \omega_0 n) + G_{n,n}^-(\omega + \omega_0 n)] \tag{21}$$

$$G_{2,1}^{(\text{el})}(\omega) = \frac{(1 - e^{-\beta\omega_0})}{2} \sum_n (-1)^n e^{-\omega_0 n\beta} [G_{n,n}^+(\omega + \omega_0 n) - G_{n,n}^-(\omega + \omega_0 n)]. \tag{22}$$

We note that the Hamiltonians (15) are tridiagonal in the Fock basis and then the inverse matrix elements are suitable to be expanded in a recursion form; an extended treatment on the inversion of tridiagonal matrices is given in [34]. In particular, the diagonal elements $G_{n,n}^\pm$ can be evaluated by a very rapidly convergent recursion obtained by the following continued fraction expansion:

$$G_{n,n}^\pm(\omega) = \frac{1}{\omega - n\omega_0 \pm J(-1)^n - \Sigma^\pm(\omega)} \tag{23}$$

where $\Sigma^\pm(\omega) = \Sigma_{\text{em}}^\pm(\omega) + \Sigma_{\text{ab}}^\pm(\omega)$ is the sum of the contribution given by the emitted and absorbed phonon. The explicit form of $\Sigma_{\text{em}}^\pm$ and $\Sigma_{\text{ab}}^\pm$ and other details are given in appendix A.

It is worth stressing that (23) is the analytical *exact* expression of the electron's Green function for any finite temperature. The continued fraction method also permits us to evaluate the eigenvectors, starting from the knowledge of the eigenvalues (i.e. the poles of any elements $G_{m,n}^\pm$) (see appendix A).

In the same way we can assess the probability distribution function for the displacement operator (10)

$$P(x) = \frac{1}{Z} \text{tr}[e^{-\beta\tilde{H}} V |x\rangle\langle x| V^{-1}]. \tag{24}$$

Recalling that $(-1)^{a^\dagger a} |x\rangle\langle x| (-1)^{a^\dagger a} = |-x\rangle\langle -x|$ we obtain

$$P(x) = \frac{1}{2Z} \sum_\alpha e^{-\beta E_\alpha^+} (|\phi_\alpha^+(x)|^2 + |\phi_\alpha^+(-x)|^2) + e^{-\beta E_\alpha^-} (|\phi_\alpha^-(x)|^2 + |\phi_\alpha^-(-x)|^2)]. \tag{25}$$

The evaluation of the polaron Green function can be done on the same footing, but the expression also involves the non-diagonal elements of the resolvent operators, causing an exponential increase of the numerical calculations.

To avoid this problem, we first perform the LF transformation and then apply, on the resulting Hamiltonian (5), a different FG transformation

$$V_1 = \frac{1}{\sqrt{2}} \begin{pmatrix} 1 & -(-1)^{a^\dagger a} \\ (-1)^{a^\dagger a} & 1 \end{pmatrix}. \tag{26}$$

The new Hamiltonian $\tilde{H}_{LF} = V_1 \bar{H} V_1^{-1}$ is

$$\bar{H}_{LF} = \begin{pmatrix} \bar{H}_+ & 0 \\ 0 & \bar{H}_- \end{pmatrix} \tag{27}$$

where

$$\bar{H}_\pm = \omega_0 a^\dagger a + J(-1)^{a^\dagger a} e^{\mp 2\alpha(a^\dagger - a)} + E_p/2 \tag{28}$$

is real and symmetric but not tridiagonal in the basis of the harmonic oscillator; the matrix elements of $\bar{H}_\pm$ are given in appendix B. In this case, a continued fraction expansion is not possible but an exact diagonalization can be done even with a very large number of phonons. The states become

$$V_1|n, j\rangle = \frac{(-1)^{nj}}{\sqrt{2}} \left((-1)^{(j-1-n)}|1\rangle + |2\rangle\right)|n\rangle. \tag{29}$$

In analogy with the case of the electron, discussed above, the polaron Green function can be expressed in terms of the resolvent

$$\bar{G}^\pm(\omega) = \langle n|\frac{1}{\omega - \bar{H}_\pm}|n\rangle \tag{30}$$

obtaining a more practical expression

$$G_{1,1}^{(pol)}(\omega) = \frac{(1 - e^{-\beta\omega_0})}{2} \sum_n e^{-\omega_0 n\beta} \left[\bar{G}_{n,n}^+(\omega + n\omega_0 + E_p/2)\right.$$
$$\left. + \bar{G}_{n,n}^-(\omega + n\omega_0 + E_p/2)\right] \tag{31}$$

$$G_{2,1}^{(pol)}(\omega) = \frac{(1 - e^{-\beta\omega_0})}{2} \sum_n (-1)^n e^{-\omega_0 n\beta} \left[\bar{G}_{n,n}^-(\omega + n\omega_0 + E_p/2)\right.$$
$$\left. - \bar{G}_{n,n}^+(\omega + n\omega_0 + E_p/2)\right]. \tag{32}$$

Spectral function can be defined for both electron and polaron as

$$A(k, \omega) = -\frac{\text{Im}}{2\pi}(G_{1,1}(\omega) \pm G_{2,1}(\omega)) \tag{33}$$

where the + sign is taken for the reciprocal lattice vector $k = 0$ and − for $k = \pi$.

4. Results

At finite temperatures, the polaron crossover moves toward larger value of the coupling due to the increasing importance of thermal fluctuations as can be seen from figure 1. At large temperatures $T/J \gg \gamma$ the adiabatic result is approached. The $\gamma = 0$ crossover line can be obtained analytically, exploiting the bimodality condition for $P(x)$. In the adiabatic limit we get from (12)

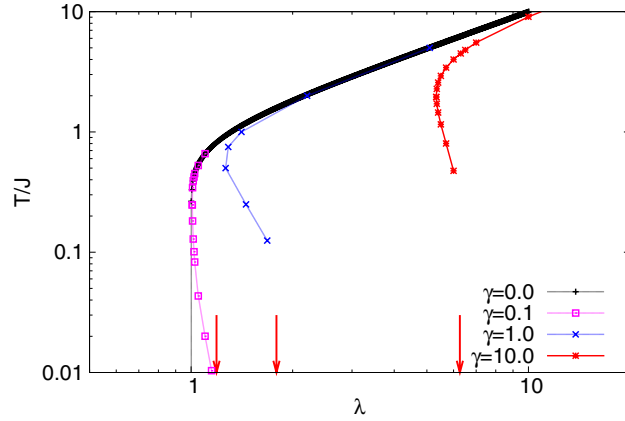$$P(x) \propto \exp(-E_r^-/T) + \exp(-E_r^+/T). \tag{34}$$

Figure 1. Lines separating monomodality (on the left) from bimodality (on the right) of $P(x)$. Arrows indicate the $T = 0$ crossover point.

The crossover temperature T_x can be obtained from the relation $d^2 P(x)/dx^2 > 0$ at $x = 0$, giving

$$T_x = \frac{J}{\tanh^{-1}(1/\lambda)}. \tag{35}$$

A crude estimation of the crossover temperature can be done comparing the polaronic displacement x_0 and the thermally induced fluctuations which gives asymptotically $T_x \simeq J\lambda$.

Quantum fluctuations are only effective for $T/J < \gamma$; they shift the polaron crossover toward larger values of λ. Notice a re-entrance of T_x which is present for all displayed values of γ. This phenomenon is rather general [35] and can be ascribed to the relevance of quantum fluctuations as far as $T/J < \gamma$, leading to a stabilization of the non-polaronic character of the phononic wavefunction.

Now let us examine the spectral functions as given by equations (21), (22), (31) and (32) in the various regimes. We start with the anti-adiabatic case $\gamma \gg 1$ in weak (figure 2 lower panel) and strong coupling (figure 2 upper panel). In this figures we have chosen a large Lorentzian broadening to show the overall distribution of the spectral weight.

In both weak and strong coupling, we notice that, as temperature increases, electron spectral function becomes rapidly broad, while polaron spectral function remains peaked around ground state energy. The difference between weak and strong coupling is evident at low temperature, where the distribution of the electronic spectral weight has the well known Poissonian shape, centred at the polaron energy from the ground state. Notice that the small resonances which appear at twice the polaronic energy in the polaron Green function are effects of the hopping term J since for $J = 0$ the polaron Green function is single peaked at $\omega = E_p$.

In figure 3, the polaronic band, i.e. the peak at E_p in figure 2, is resolved, using a smaller Lorentzian broadening, in weak (lower panel) and strong (upper panel) coupling. Here, the effects of temperature are evident in both electron and polaron DOS, but in a different way at small and large couplings. At small coupling thermal fluctuations excite poles *inside* the zero temperature band (marked by the vertical lines in figure 3). In this regime, the $T = 0$ bandwidth is accurately predicted by the HLFA. As temperature increases HLFA predicts band *narrowing*. This behaviour is reproduced by the data through a redistribution of the spectral weight inside the $T = 0$ band.
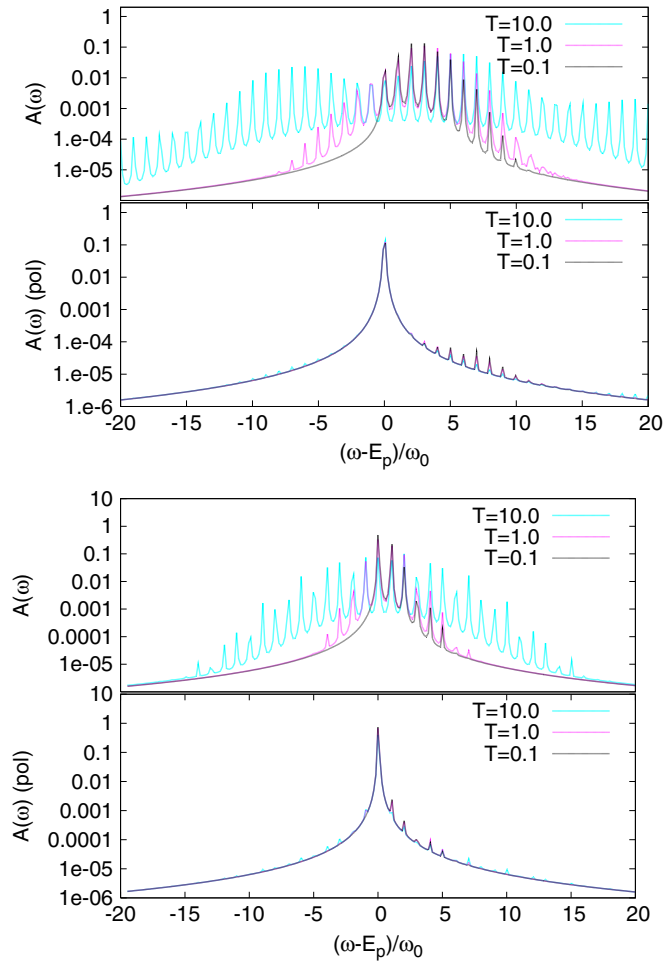
Figure 2. Electron and polaron DOS for $\gamma = 10.0$ and $\lambda = 40$ (top panels) $\lambda = 10$ (bottom panels). A Lorentzian broadening $\delta = 2J$ has been used. The polaronic spectra is essentially temperature independent.

In contrast, at strong coupling (figure 3 upper panel) the low energy bandwidth seems to *increase* rather than decrease as predicted by the HLFA. This is a general behaviour since it was also found solving an infinite lattice problem using dynamical mean field theory (DMFT) [8]. However, we shall notice that the correct interpretation of Holstein's results is that the coherence of the polaron band is lost as long as the temperature increases. Further to DMFT results, this statement must be interpreted as the coherence of the low energy states decreasing with the temperature. This does not imply that the *total* bandwidth, i.e. the bandwidth of the coherent and incoherent states, decreases. It rather increases as temperature increases [8]. The mechanism of excitation of low energy poles can be understood from the continuous fraction expansion (A.2), (A.3) of the Green function (23). In the $J = 0$ limit, from (4), the zero temperature spectral function shows typical multiphonon resonances of order m at $E_m = E_p/2 + \omega_0 m$. At non-zero temperature, absorption processes of order n, taken into account by Σ_{abs} in (23), imply excitation of resonances at energies $E_m - n\omega_0$ from the mth polaronic peak. This is an excitation of a state with m phonons which absorbs n phonons from
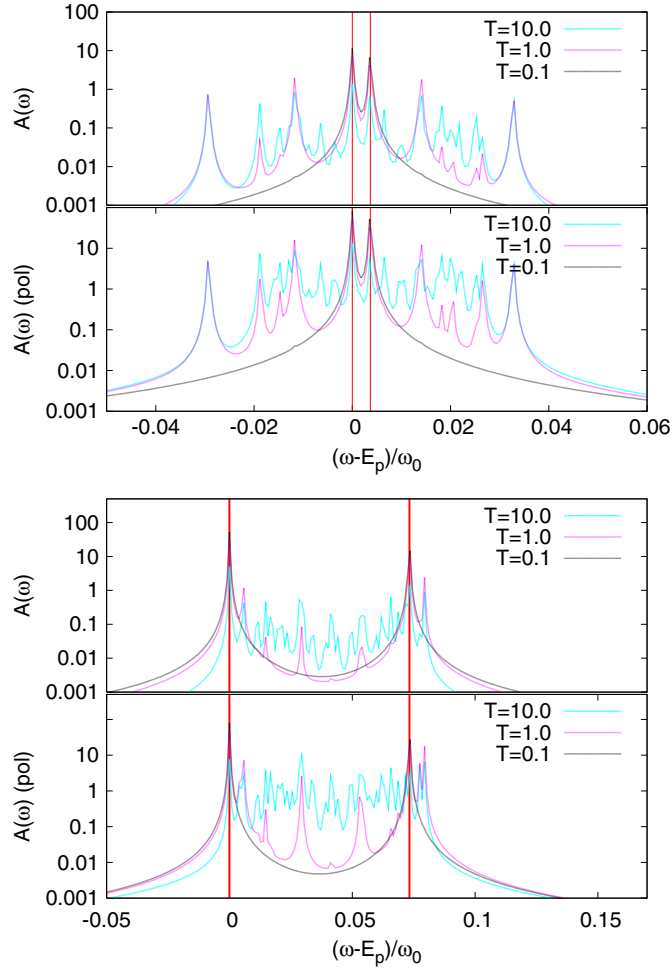
Figure 3. The polaronic band varying temperature for $\gamma = 10.0$ and $\lambda = 40$ (top panels) $\lambda = 10$ (bottom panels). A Lorentzian broadening $\delta = 0.04J$ has been used. The contribution of $k = 0$ and $k = \pi$ peaks to the total DOS is marked by vertical lines.

the bath. When $n = m$ (and $n \neq 0$) this is a thermal contribution to the polaronic 'band'. For small hopping, an m phonon band, absorbing m phonons from the bath, do not contribute to a pole exactly located at E_0 but rather *around* E_0, as can be seen in equations (21) and (22) and from equations (31) and (32). As the temperature goes up the number of such excitations increases as shown in figure 3.

Even in this case, the perturbative picture can help us to understand the mechanism better. The electron spectral functions can be perturbatively calculated (see appendix C)

$$G_{1,1}^{(el)}(\omega) \simeq \sum_{n,m} \frac{e^{-\beta\omega_0 n}}{2Z} f_{m,n}^2(-\alpha) \left[\frac{1}{\omega - \omega_0(m-n) - Jf_{m,m}(2\alpha) + \frac{g^2}{2\omega_0}} \right.$$

$$\left. + \frac{1}{\omega - \omega_0(m-n) + Jf_{m,m}(2\alpha) + \frac{g^2}{2\omega_0}} \right] \tag{36}$$

$$G_{1,2}^{(el)}(\omega) \simeq \sum_{n,m} \frac{e^{-\beta\omega_0 n}}{2Z} f_{m,n}^2(\alpha) \left[\frac{-1}{\omega - \omega_0(m-n) - J f_{m,m}(2\alpha) + \frac{g^2}{2\omega_0}} \right.$$
$$\left. + \frac{1}{\omega - \omega_0(m-n) + J f_{m,m}(2\alpha) + \frac{g^2}{2\omega_0}} \right]. \tag{37}$$

Starting from the poles of (36) and (37), it is clear that the incoherent contributions to the low energy band can be estimated by $\tilde{J}_m$, given in (11). The broadening of the band depends on whether this contribution falls outside or inside the initial band. By an asymptotic expansion of the Laguerre polynomials, it is easy to see that, for $x \simeq 0$,

$$|L_n(x)| \simeq \left| 1 - \frac{2n+1}{2} x \right| \tag{38}$$

and $|L_n(x)| < L_0(x) = 1$. So, for sufficiently small α, we have $\tilde{J}_m < \tilde{J}_0$: each contribution falls inside the band, the width of which remains the same. In the other asymptotic case,

$$|L_n(x)| \simeq \frac{|x|^n}{n!} > 1 \tag{39}$$

so, for large α, $\tilde{J}_m > \tilde{J}_0$ and the band broadens. We should stress that an average electron kinetic energy increasing with temperature has been found within the same model by Ranninger and De Mello [14]. However, low energy spectral properties and average values are not directly related, especially when only a small amount of the total spectral weight is contained in the low frequency part of the spectrum.

As a conclusion, in the strong coupling adiabatic regime, the notion of a well defined polaronic band is lost as can be seen from figure 4. Notice that by increasing temperature, electron and polaron DOS tend to have the same shape, which is entirely determined by thermal fluctuations.

The zero-temperature behaviour can be analytically explained starting by a continued fraction expansion in the strong coupling limit (appendix D)

$$A(\omega) = \frac{1}{J\sqrt{\pi\lambda\gamma}} \frac{e^{-\frac{\omega^2-1}{\gamma\lambda}}}{\sqrt{\omega^2-1}} \Theta(|\omega|-1) \tag{40}$$

with

$$\nu = \frac{xg\sqrt{2m\omega_0}}{2J}. \tag{41}$$

This result is equivalent to the adiabatic approximation [36]; indeed, (40) can be obtained by averaging a Green's function, at a given displacement x, over all possible displacements, weighted with a Gaussian phonon distribution. It is worth noticing that we here recover the adiabatic result as a limit of an exact formula.

Equation (40) gives two symmetric bands separated by a gap and having Gaussian tails induced by phonon fluctuations [37]. Compared with the $T = 0.1$ exact result in figure 4, the approximation well reproduces the higher energy band while it is less accurate for the lower energy band where some poles are present within the bandgap predicted by the adiabatic approximation.

5. Conclusions

In this work we have studied the spectral properties of the two-site Holstein model. We have also studied the polaron crossover looking at the thermal phonon distribution $P(x)$. By means
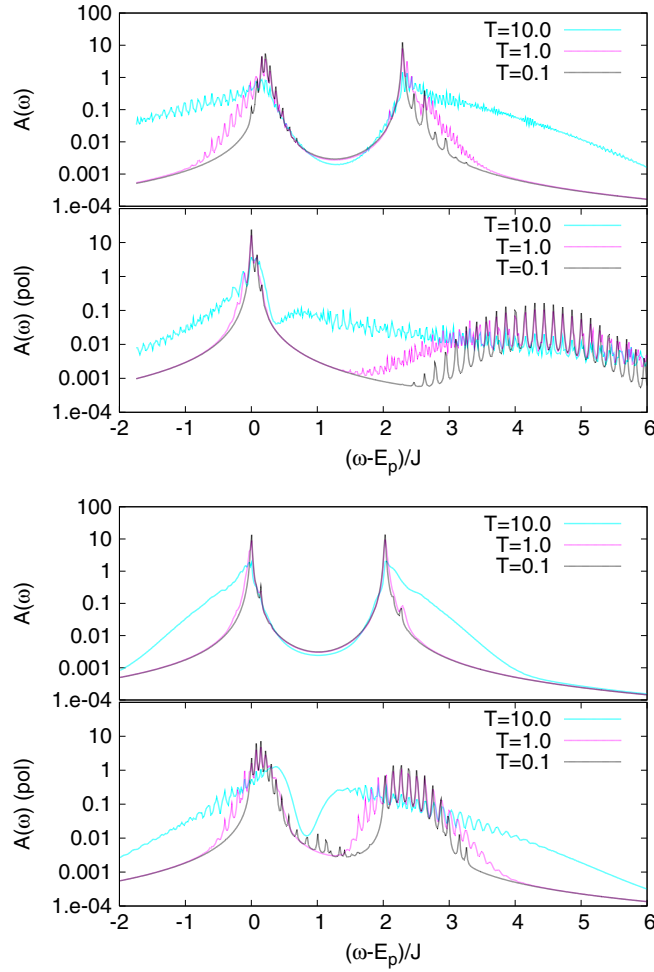
Figure 4. Electron and polaron DOS $\gamma = 0.1$ and $\lambda = 2$ (top panels) $\lambda = 0.5$ (bottom panels). A Lorentzian broadening $\delta = 0.1 J$ has been used.

of a generalization of the Fulton–Gouterman transformation, the phonon and electron degrees of freedom are separated and it is possible to obtain exact analytical results at both zero and finite temperatures and for any coupling strength.

Polaron crossover, identified by means of bimodality in $P(x)$, strongly depends on the adiabaticity ratio γ. In the adiabatic regime $\gamma < 1$ quantum fluctuations are effective when temperature is lower than the phonon frequency, leading to a shift of the crossover toward larger coupling. Generally speaking, we found that phonon distribution behaviour, within the two-site model, bears a strong resemblance to that found in an infinite size lattice, e.g. by DMFT analysis [38, 35]. The essential features captured by the two-site model is, in this case, the competition between hopping and localization due to local interaction with phonon. The fact that in an extended model electron the spectrum is continuous does not seems to be qualitatively important for the behaviour of $P(x)$.

In contrast, the electron spectrum of an infinite lattice is very different from that of a two-site model. Nonetheless, some overall features are also present in our case. First of all,

we found that the validity of the HLFA for the polaron bandwidth is restricted to the low temperature anti-adiabatic regime, as was also found in the infinite lattice case [8]. This is the case in which, at low temperature, the charge behaves as a coherent polaron, as we have demonstrated by comparing the electron and polaron Green function. On the other hand, in the adiabatic case, the polaron is highly incoherent. The HLFA approximation well works at large temperatures in weak coupling also. Here, the shrinking of the polaron band, predicted by this theory, is found in a two-site system as the emergence of poles inside the $k = 0$ $k = \pi$ two-site band.

On the other hand, at strong coupling, contrary to Holstein's prediction, no low energy 'band' shrinking has been observed, while an increasing of it seems to occur by increasing the temperature. The broadening of the low energy bands is revealed in the two-site model as a spectral weight spreading over an increasing number of poles, but has also been found in an extended system studied with DMFT [39]. Such a broadening observed in the spectral function also has a deep impact in transport properties [40], where it rules the temperature at which activation processes dominate the transport [40].

We have explained the band broadening in terms of the continued fraction expansion as an effect due to the presence of a finite hopping on the thermal absorption of phonons. We guess that the Holstein's results must be interpreted in terms of coherence of states rather than band amplitude. To quantify this conjecture we must measure a degree of coherence for a two-level system coupled to a phonon. Work in this direction is currently in progress.

Acknowledgments

Appendix A. Continued fraction expansion

It can be proved [41, 34] that the elements of the inverse of a tridiagonal matrix have a continued fraction form. This result is commonly used to evaluate the resolvent operator of a tridiagonal Hamiltonian [42, 8, 17]. The advantage is that the recursion formula obtained is rapidly convergent and no diagonalization has to be done. In particular, the Hamiltonian (15) is tridiagonal in the Fock basis and every element of the resolvent (20) can be evaluated. In our case, we are interested only in the diagonal elements whose continued fraction expression is

$$G_{n,n}^{\pm}(\omega) = \frac{1}{\omega - n\omega_0 \pm J(-1)^n - \Sigma_{\text{em}}^{\pm} - \Sigma_{\text{ab}}^{\pm}} \tag{A.1}$$

where Σ_{em} and Σ_{ab} are, respectively, the self-energy contribution from the emitted and absorbed phonons; they can be expressed again as a continued fraction

$$\Sigma_{\text{em}}^{\pm} = \cfrac{(n+1)\tilde{g}^2}{\omega - (n+1)\omega_0 \pm J(-1)^{n+1} - \cfrac{(n+2)\tilde{g}^2}{\omega - (n+2)\omega_0 \pm J(-1)^{n+2} - \cfrac{(n+3)\tilde{g}^2}{\omega - (n+3)\omega_0 \mp J(-1)^{n+3} - \cdots}}} \tag{A.2}$$

$$\Sigma_{\text{ab}}^{\pm} = \cfrac{n\tilde{g}^2}{\omega - (n-1)\omega_0 \pm J(-1)^{n-1} - \cfrac{(n-1)\tilde{g}^2}{\omega - (n-2)\omega_0 \pm J(-1)(n-2) - \cfrac{(n-2)\tilde{g}^2}{\ddots - \cfrac{\tilde{g}^2}{\omega \pm J(-1)}}}} \tag{A.3}$$

or in the recursive form

$$\Sigma_{\text{em},p}^{\pm} = \frac{(n+p)\tilde{g}^2}{\omega + (-(n+p)\omega_0 \pm (-1)^{n+p}J) - \Sigma_{\text{em},p+1}^{\pm}} \tag{A.4}$$

$\Sigma_{\text{em}}^{\pm} = \Sigma_{\text{em},1}^{\pm}$

$$\Sigma_{\text{ab},p}^{\pm} = \frac{(n-p)\tilde{g}^2}{\omega + (-(n-p-1)\omega_0 \pm (-1)^{n-p-1}J) - \Sigma_{\text{ab},p+1}^{\pm}} \tag{A.5}$$

$\Sigma_{\text{ab}}^{\pm} = \Sigma_{\text{ab},0}^{\pm}$ and $\Sigma_{\text{ab},n+1}^{\pm} = 0$.

Both (A.2) and (A.3) can be expressed in the compact form

$$\Sigma_p^{\pm} = \frac{b_p}{\omega + a_p^{\pm} - \Sigma_{p+1}^{\pm}}. \tag{A.6}$$

This recursion rule can be used to evaluate the coefficients $\gamma_{\alpha,n}^{\pm}$ introduced in (19). Consider the equation (A.1). Let ω^* be one of the poles of the function, the self-energy can be expanded around it

$$G_{n,n}(\omega) \simeq \frac{1}{(\omega - \omega^*)(1 - z_{\text{em}}^{\pm}(\omega^*) - z_{\text{ab}}^{\pm}(\omega^*))} \tag{A.7}$$

where $z = \frac{\partial \Sigma}{\partial \omega}$. So the weight for the pole is

$$\gamma_{k,n}^{\pm} \simeq \frac{1}{1 - z_{\text{em}}^{\pm}(\omega_k^{\pm}) - z_{\text{ab}}^{\pm}(\omega_k^{\pm})}. \tag{A.8}$$

Using (A.6) it is possible to estimate the derivate by another linearization

$$\Sigma_p^{\pm}(\omega) \simeq \frac{b_p}{(\omega - \omega^*)(1 - z_{p+1}^{\pm}(\omega^*)) + \omega^* + a_p^{\pm} - \Sigma_{p+1}^{\pm}(\omega^*)} \tag{A.9}$$

$$z_p^{\pm} = \frac{(z_{p+1}^{\pm}(\omega^*) - 1)b_p^{\pm}}{(\omega^* + a_p^{\pm} - \Sigma_{p+1}^{\pm}(\omega^*))^2}. \tag{A.10}$$

Appendix B. Displacement operator in the Fock basis

In the Fock basis the displacement matrix elements $\langle m|e^{\alpha(a^{\dagger}-a)}|n\rangle = f_{n,m}(\alpha)$ are [43–45], for $m \geqslant n$,

$$f_{n,m}(\alpha) = \frac{e^{-\frac{\alpha^2}{2}}\sqrt{n!m!}}{(m!)} L_n^{m-n}(\alpha^2)\alpha^{m-n} \tag{B.1}$$

where $L_{\bar{n}}^s(\alpha^2)$ is an associated Laguerre polynomial

$$L_a^b(x) = \sum_{k=0}^{a} \frac{(-1)^k(a+b)!}{(a-k)!(b+k)!k!}x^k; \tag{B.2}$$

taking into account that $f_{n,m}(\alpha) = f_{m,n}(\alpha)$, the matrix is completely defined. From this result it is possible to express the matrix element of the Hamiltonian (28)

$$\langle m|\bar{H}_{\mp}|n\rangle = \omega_0 n\delta_{n,m} \pm J(-1)^m f_{n,m}(\pm 2\alpha). \tag{B.3}$$

Appendix C. First order perturbative expansion in J

Starting from the atomic Hamiltonian (4) we introduce the hopping contribution in (5) as a perturbation

$$\bar{H}_I = -J(c_1^\dagger c_2 e^{2\alpha(a^\dagger - a)} + \text{h.c.}).\tag{C.1}$$

The zeroth order correction for the eigenstates and the first order for the energies is obtained by diagonalizing the matrix

$$-J \begin{pmatrix} 0 & \langle n|e^{2\alpha(a^\dagger - a)}|n\rangle \\ \langle n|e^{-2\alpha(a^\dagger - a)}|n\rangle & 0 \end{pmatrix}.\tag{C.2}$$

The first order energy expansion is

$$E_n^\pm \simeq \omega_0 n - \frac{g^2}{2\omega_0} \pm Jf_{n,n}(2\alpha)\tag{C.3}$$

where $f_{n,n}(2\alpha)$ is given in (B.1). The zeroth order eigenstates are

$$|\bar{\psi}_n^\pm\rangle_{(0)} = \frac{1}{\sqrt{2}} (|1\rangle \mp |2\rangle)\, |n\rangle\tag{C.4}$$

and the first order correction is

$$|\bar{\psi}_n^\pm\rangle_{(1)} = -\frac{J}{\sqrt{2}} \sum_{k \neq n} \frac{\mp f_{n,k}(2\alpha)|1\rangle + f_{n,k}(-2\alpha)|2\rangle}{\omega_0(n-k)} |k\rangle\tag{C.5}$$

so that

$$|\bar{\psi}_n^\pm\rangle \simeq \frac{1}{N^\pm} \left[|\bar{\psi}_n^\pm\rangle_{(0)} + |\bar{\psi}_n^\pm\rangle_{(1)} \right]\tag{C.6}$$

where $N^\pm$ is a suitable normalization.

The electronic Green's functions can be estimated first performing an LF transformation

$$G_{1,1}^{(\text{el})}(\omega) = \sum_n \frac{e^{-\beta\omega_0 n}}{Z} \langle n|c_1 D_R \frac{1}{\omega - H_{\text{LF}} + \omega_0 n} D_R^\dagger c_1^\dagger|n\rangle\tag{C.7}$$

$$G_{1,2}^{(\text{el})}(\omega) = \sum_n \frac{e^{-\beta\omega_0 n}}{Z} \langle n|c_2 D_R \frac{1}{\omega - H_{\text{LF}} + \omega_0 n} D_R^\dagger c_1^\dagger|n\rangle,\tag{C.8}$$

where $D_R = e^{\alpha(c_1^\dagger c_1 - c_2^\dagger c_2)(a^\dagger - a)}$, and then using equations (C.3)–(C.5). In the Lehman representation we have

$$G_{1,1}^{(\text{el})}(\omega) = \sum_{n,m} \frac{e^{-\beta\omega_0 n}}{Z} \left[\frac{|\langle n|e^{-\alpha(a^\dagger - a)}c_1|\bar{\psi}_m^+\rangle|^2}{\omega - E_m^+ + \omega_0 n} + \frac{|\langle n|e^{-\alpha(a^\dagger - a)}c_1|\bar{\psi}_m^-\rangle|^2}{\omega - E_m^- + \omega_0 n} \right]\tag{C.9}$$

$$G_{1,2}^{(\text{el})}(\omega) = \sum_{n,m} \frac{e^{-\beta\omega_0 n}}{Z} \left[\frac{\langle n|e^{\alpha(a^\dagger - a)}c_2|\bar{\psi}_m^+\rangle\langle\bar{\psi}_m^+|e^{\alpha(a^\dagger - a)}c_1^\dagger|n\rangle}{\omega - E_m^+ + \omega_0 n} \right.$$

$$\left. + \frac{\langle n|e^{\alpha(a^\dagger - a)}c_2|\bar{\psi}_m^-\rangle\langle\bar{\psi}_m^-|e^{\alpha(a^\dagger - a)}c_1^\dagger|n\rangle}{\omega - E_m^- + \omega_0 n} \right]\tag{C.10}$$

and, taking into account that

$$\langle n|e^{-\alpha(a^\dagger - a)}c_1|\bar{\psi}_m^\pm\rangle = \frac{1}{N^+} \left[f_{m,n}(-\alpha) \pm J \sum_{k \neq m} \frac{f_{m,k}(2\alpha)f_{k,n}(-\alpha)}{\omega_0(m-k)} \right]\tag{C.11}$$

$$\langle n|e^{\alpha(a^\dagger - a)}c_2|\bar{\psi}_m^\pm\rangle = \frac{1}{N^-} \left[\mp f_{m,n}(\alpha) - J \sum_{k \neq m} \frac{f_{m,k}(-2\alpha)f_{k,n}(\alpha)}{\omega_0(m-k)} \right],\tag{C.12}$$

we obtain equations (36) and (37).

Appendix D. Electron Green's functions. Adiabatic strong coupling limit

In the limit $\omega_0 \to 0$ and $\lambda \to \infty$, starting from the continued fraction expansion (A.1), we have

$$G_{0,0}^{\pm} = (\omega \pm J)F(\omega) \tag{D.1}$$

with

$$F(\omega) = \cfrac{1}{\omega^2 - J^2 - \cfrac{\tilde{g}^2(\omega^2 - J^2)}{\omega^2 - J^2 - \cfrac{2\tilde{g}^2(\omega^2 - J^2)}{\omega^2 - J^2 - \cfrac{3\tilde{g}^2(\omega^2 - J^2)}{\cdots}}}}. \tag{D.2}$$

For $T = 0$ the electron Green's function is

$$G_{1,1}(\omega) = \omega F(\omega). \tag{D.3}$$

It can be shown [46] that

$$\int_{\infty}^{\infty} \frac{d\epsilon}{\sqrt{2\pi}} \frac{e^{-\epsilon^2}}{z - \epsilon} = \cfrac{1}{\sqrt{2}z - \cfrac{1}{\sqrt{2}z - \cfrac{2}{\sqrt{2}z - \cfrac{3}{\cdots}}}} = \cfrac{b}{\sqrt{2}zb - \cfrac{b^2}{\sqrt{2}zb - \cfrac{2b^2}{\sqrt{2}zb - \cfrac{3b^2}{\cdots}}}}; \tag{D.4}$$

making the substitutions

$$b = \tilde{g}\sqrt{\omega^2 - J^2} \tag{D.5}$$
$$\sqrt{2}zb = \omega^2 - J^2 \tag{D.6}$$

we obtain

$$F(\omega) = \frac{1}{\sqrt{\omega^2 - J^2}} F(\omega) \int_{\infty}^{\infty} \frac{d\epsilon}{\sqrt{\pi}} \frac{e^{-\epsilon^2}}{\sqrt{\omega^2 - J^2} - \tilde{g}\sqrt{2}\epsilon}; \tag{D.7}$$

the Green's function becomes

$$G_{1,1}(\omega) = \frac{\omega}{J\sqrt{\pi\lambda\gamma}} \int_{-\infty}^{\infty} d\nu\, e^{-\frac{\nu^2}{\gamma\lambda}} \frac{1}{\omega^2/J^2 - 1 - \nu^2} \tag{D.8}$$

with ν given in (41).

References

[1] Tiablikov S V 1952 *Zh. Eksp. Teor. Fiz.* **23** 381
[2] Holstein T 1959 *Ann. Phys.* **8** 325
    Holstein T 1959 *Ann. Phys.* **8** 343
[3] Heeger A J, Kivelson S, Schrieffer J R and Su W P 1988 *Rev. Mod. Phys.* **60** 781
[4] Silinsh E A and Ćapek V 1994 *Organic Molecular Crystals: Interaction, Localization, and Transport Phenomena* (Woodbury: AIP)
    For transport phenomena see also the review paper de Boer R W I, Gershenson M E, Morpurgo A F and Podzorov V 2004 *Preprint* cond-mat/0404100
[5] Damjanović A, Kosztin I, Kleinekathöfer U and Schulten K 2002 *Phys. Rev.* E **65** 031919
[6] see for instance Endres R G, Cox D L and Singh R R P 2004 *Rev. Mod. Phys.* **76** 195
[7] Zhang W, Govorov A O and Ulloa S E 2003 *Phys. Rev.* B **66** 060303(R)
[8] Ciuchi S, de Pasquale F, Fratini S and Feinberg D 1997 *Phys. Rev.* B **56** 4494
[9] Alexandrov A S, Kabanov V V and Ray D K 1994 *Phys. Rev.* B **49** 9915
[10] Feinberg D, Ciuchi S and de Pasquale F 1990 *Int. J. Solid State* B **4** 1317
[11] Firsov Yu A and Kudinov E K 1997 *Phys. Solid State* **39** 1930
[12] Rongsheng H, Zijing L and Kelin W 2002 *Phys. Rev.* B **65** 174303
[13] Zijing L, Rongsheng H and Kelin W 2003 *Int. J. Mod. Phys.* B **17** 4252
[14] de Mello E V L and Ranninger J 1997 *Phys. Rev.* B **55** 14872

[15] de Mello E V L and Ranninger J 1998 *Phys. Rev.* B **58** 9098
[16] Swain S 1973 *J. Phys. A: Math. Gen.* **6** 192
[17] Capone M and Ciuchi S 2002 *Phys. Rev.* B **65** 104409
[18] Acquarone M, Iglesias J R, Gusmão M A, Noce C and Romano A 1998 *Phys. Rev.* B **58** 7626
[19] Lang I G and Firsov Yu A 1968 *Sov. Phys.—Solid State* **9** 2701
     Kudinov E K and Firsov Yu A 1965 *Sov. Phys.—Solid State* **7** 435
[20] Kotliar G, Savrasov S Y, Palsson G and Biroli G 2001 *Phys. Rev. Lett.* **87** 186401
     Maier T, Jarrell M, Pruschke T and Keller J 2000 *Eur. Phys. J.* B **13** 613
[21] Rivier N and Coe T J 1977 *J. Phys. C: Solid State Phys.* **10** 4471
[22] Lang I G and Firsov Yu A 1963 *Sov. Phys.—JETP* **16** 1301
[23] Robin J M 1997 *Phys. Rev.* B **56** 13634
[24] Egami T and Billinge S J L 2003 *Underneath the Bragg Peaks: Structural Analysis of Complex Materials*
     (Oxford: Pergamon)
[25] Millis A J, Mueller R and Shraiman B I 1996 *Phys. Rev.* B **54** 5389
[26] Appel J 1967 *Solid State Physics* ed H Ehrenreich, F Seiz and D Turnbull (New York: Academic) p 193
[27] Herfort U and Wagner M 2001 *J. Phys.: Condens. Matter* **13** 3297
[28] Ranninger J and Thibblin U 1992 *Phys. Rev.* B **45** 7730
[29] Gerlach B and Löwen H 1987 *Phys. Rev.* B **35** 4291
     Löwen H 1988 *Phys. Rev.* B **37** 8661
[30] Weiss U 1993 *Quantum Dissipative Systems* (Singapore: World Scientific)
[31] Fulton R and Gouterman M 1961 *J. Chem. Phys.* **35** 1059
[32] Wagner M and Köngeter A 1989 *Phys. Rev.* B **39** 4644
     Wagner M 1985 *J. Phys. A: Math. Gen.* **18** 1915
     Wagner M 1984 *J. Phys. A: Math. Gen.* **17** 3409
[33] Wagner M 1984 *J. Phys. A: Math. Gen.* **17** 2319
[34] Yamani H A and Abdelmonem M S 1997 *J. Phys. A: Math. Gen.* **30** 2889
[35] Capone M, Ciuchi S and Sangiovanni G 2005 *Preprint* cond-mat/0503681
[36] Rösch O and Gunnarsson O 2005 *Eur. Phys. J.* B **43** 11
[37] Fratini S and Ciuchi S 2005 *Phys. Rev.* B **72** 235107
[38] Motome Y and Kotliar G 2000 *Phys. Rev.* B **62** 12800
[39] Fratini S and Ciuchi S 2005 *Preprint* cond-mat/0512202
[40] Fratini S and Ciuchi S 2003 *Phys. Rev. Lett.* **91** 256403
[41] Viswanath V S and Müller G 1994 *The Recursion Method* (Berlin: Springer)
[42] Cini M and D'Andrea A 1988 *J. Phys. C: Solid State Phys.* **21** 193
[43] Herfort U 2000 *PhD Thesis* Institut für Theoretische Physik der Universität Stuttgart
[44] Cahill K E and Glauber R J 1969 *Phys. Rev.* **177** 1882
[45] Richter T 1996 *Phys. Rev.* A **53** 53
[46] Abramovitz M and Stegun I A 1964 *Handbook of Mathematical Functions* (New York: Dover)